NMR analysis of secondary structure and dynamics of a recombinant peptide from the N-terminal region of human erythroid α-spectrin

Sunghyouk Park[a], Michael E. Johnson[a,*], L.W.-M. Fung[b,1]

[a] *Center for Pharmaceutical Biotechnology, 900 S. Ashland Avenue-mc 870, Chicago, IL 60607-7173, USA*
[b] *Department of Chemistry, Loyola University of Chicago, 6525 N. Sheridan Road, Chicago, IL 60626, USA*

Received 20 June 2000; revised 2 October 2000; accepted 9 October 2000

First published online 3 November 2000

Edited by Thomas L. James

Abstract We have studied the nuclear magnetic resonance solution secondary structure of the N-terminal region in human erythroid α-spectrin using a recombinant model peptide of α-spectrin consisting of residues 1–156. Pulsed field gradient diffusion coefficient measurements show that the model peptide exists as a monomer under the solution conditions used. The first 20 residues are in a random coil conformation, followed by a helix of 25 residues and then a random coil segment before the next helix. The random coil nature of this linker was confirmed by the presence of fast internal motion from ^{15}N relaxation measurements. The second, third and fourth helices are thought to form the triple helical bundle structural domain, consistent with previous studies. Our study shows that the N-terminal region of α-spectrin prior to the first structural domain forms a well behaved helix without its β-spectrin partner.

Key words: Human erythrocyte spectrin; Nuclear magnetic resonance; Secondary structure; Tetramerization region

1. Introduction

Spectrin, a member of the actin binding protein family, is present in such diverse tissues as erythrocytes [1], skin [2] and brain [3]. The major role of erythroid spectrin is to provide mechanical support to the cytoplasmic membrane by forming a protein network under the membrane bilayer [4–6].

In the erythrocyte, spectrin is thought to be largely responsible for the unique biconcave shape of the cell, and for the remarkable stability and elasticity of the membrane which withstands the large shearing forces encountered during microcirculation. Spectrin is composed of two subunits – α (280 kDa) and β (246 kDa) – which associate laterally to form dimers and functional heterotetramers ($\alpha_2\beta_2$). Each subunit consists of multiple homologous sequence motifs of about 106 amino acid residues [7] that form a triple helical coiled coil structural domain. This structural domain is believed to be a common feature in all members of the spectrin superfamily [8]. However, we have shown that peptides with more than one domain are needed to mimic the structural stability of erythroid spectrin [9].

Despite the functional and structural similarities among members in the spectrin family, specific differences have also been noted, especially between erythrocyte and non-erythrocyte spectrins. Additional structural domains such as the plekstrin homology domain [10], and a calmodulin binding domain [11] are present in brain spectrin, but not in erythrocyte spectrin. Brain and erythrocyte spectrin also have different calcium affinities, suggesting the possibility of different roles for calcium with these molecules [12]. Thus, it is possible that specific differences may also exist in the structure of the general triple helical structural domain in different types of spectrins. No experimental information on the structure of human erythroid spectrin has been reported.

The N-terminal region of human erythrocyte α-spectrin (αN) and the C-terminal region of β-spectrin (βC) are involved in spectrin tetramer formation, with dissociation constants in the μM range [13], and the αN/βC association region is often called the tetramerization site. Spectrin tetramers play a critical role in maintaining the architecture, and therefore the integrity, of the red cell membrane. Many hereditary hemolytic anemias involve spectrin mutations that destabilize tetramer formation [14]. Many mutations lie in or near the tetramerization sites in either α- or β-spectrin [14].

Since about 30 residues in the αN region are homologous to the sequence of the third helix, and about 60 residues in the βC region are homologous to the sequence of the first two helices in the structural domain, it has been suggested that these helices in the αN and βC regions associate to form a triple helical bundle similar to the 106-amino acid structural domains [15]. However, there is no direct experimental evidence for the proposed conformation.

We have shown that a series of spectrin recombinant peptides are good model systems for studies of the α-spectrin N-terminus [16]. We have also previously determined that residues 52–156 form the first structural domain in α-spectrin [17] and have recently assigned the backbone nuclear magnetic resonance (NMR) resonances for Spα1–156[1], a recombinant peptide consisting of the first 156 residues of α-spectrin [18].

Our NMR results for this peptide show that (1) the erythrocyte spectrin structural domain exhibits a conformation largely consistent with the triple helical bundle structure in

*Corresponding author. Fax: (1)-312-413 9303.
E-mail: mjohnson@uic.edu

[1] Also corresponding author. Fax: (1)-773-508 3086;
E-mail: lfung@luc.edu

Abbreviations: Spα1–156, recombinant peptide comprising the first 156 residues of α-spectrin; PFGSE, pulsed field gradient spin echo; NOESY, nuclear Overhauser enhancement spectroscopy; HSQC, heteronuclear single quantum-correlation spectroscopy; HNCA, amide proton to nitrogen to α-carbon correlation; T_1, longitudinal relaxation time; T_2, transverse relaxation time

0014-5793/00/$20.00
PII: S0014-5793(00)02186-4

chicken brain and *Drosophila* spectrin [19,20], and (2) the region prior to the structural domain consists of a well defined helical conformation even in the absence of β-spectrin, and is connected to the structural domain by a random coil linker. It is hoped that understanding the conformation of this region may provide insight toward the pathology and physiology of spectrin tetramerization.

2. Materials and methods

2.1. NMR sample preparation

The peptide Spα1–156, unlabeled or labeled with ^{15}N, was prepared as before [18], and NMR samples (1 mM) were prepared in 5 mM phosphate buffer (pH 6.5) with 95% H_2O and 5% D_2O containing 150 mM NaCl and 0.01% NaN_3. Precipitation was found in some samples at lower NaCl concentrations over an extended period during NMR experiments. All spectra were obtained at 20°C.

2.2. Translational self-diffusion coefficient measurements

Translational self-diffusion coefficients (D_T) from pulsed field gradient spin echo (PFGSE) NMR experiments [21,22] were used to assess the oligomeric status of Spα1–156 in solution. The diffusion delay (Δ) was fixed to 150 ms, and the gradient pulse duration (δ) to 7.5 ms. The signal intensity (S) was measured in a series of experiments as the gradient strength (G) was varied linearly from 2 to 96% of the maximum value. D_T was calculated by a least square fit of the normalized signal decay (S/S_0) to the equation: $S/S_0 = \exp[-(\gamma G\delta)^2 D_T(\Delta-\delta/3)]$, where γ is the gyromagnetic ratio [22]. Diffusion data were acquired on a Bruker DRX-500 with a single z-axis gradient probe. At least three different resonances were used for the calculation of the diffusion coefficient for Spα1–156, and averaged values were calculated. For comparison, measurements were also obtained on lysozyme and carbonic anhydrase, two proteins that are known to exist as monomers in solution.

2.3. NMR spectroscopy

All NMR spectra were recorded on 600 MHz spectrometers (Bruker DRX-600 or Bruker DMX-600) with triple resonance, triple axis gradient probes. In addition to those spectra acquired for the previously reported resonance assignments [18], additional spectra were obtained to study the secondary structure and dynamics. Heteronuclear ^1H–^{15}N nuclear Overhauser enhancement (NOE), ^{15}N-transverse relaxation time (T_2) and ^{15}N-longitudinal relaxation time (T_1) spectra were acquired using published pulse sequences [23] with a water flip-back pulse. For ^1H–^{15}N NOE measurements, two intercalated 2D-heteronuclear single quantum-correlation spectroscopy (HSQC) were acquired with and without ^1H saturation, with 256 ^{15}N points and 80 scans per t_1 increment. ^1H saturation was implemented using a 120° ^1H pulse train with 5 ms intervals. For T_2 measurements, a series of experiments was performed with nine different relaxation delays (8.16, 16.3, 24.5, 32.6, 49, 73.4, 97.9, 122.4, and 171.4 ms) using the ^{15}N Carr–Purcell–Meiboom–Gill pulse train [23].

For T_1 measurements, a series of experiments were conducted with eight different relaxation delays (0.012, 0.072, 0.132, 0.232, 0.392, 0.612, 0.992, and 1.492 s). A series of ^1H off-resonance 180° pulses was applied at 5 ms intervals to suppress cross correlation during the relaxation delay.

2.4. Data analysis

Raw data were processed and analyzed using the Felix 97.0 software (MSI, San Diego, CA, USA). NOE values were calculated from the ratios of peak intensities on spectra with (I_{sat}) and without proton saturation (I_{unsat}). The standard deviations in NOE values (σ_{noe}) were estimated from the equation, $\sigma_{noe}/NOE = \{(\sigma_{sat}/I_{sat})^2+(\sigma_{unsat}/I_{unsast})^2\}^{1/2}$ [23]. σ_{sat} and σ_{unsat} are the standard deviation values of peak intensities with and without saturation, respectively, and were calculated from the rms noise of the blank region. T_1 and T_2 relaxation times were calculated by non-linear least square fits of signal decays to an exponential decay function, $S/S_0 = \exp(-t/T_{1,2})$ [23]. The uncertainties of the T_1 and T_2 values were obtained as reported previously [24,25]. ^1H–^{15}N heteronuclear NOE values and ^{15}N-relaxation rates ($R_1 = T_1^{-1}$ and $R_2 = T_2^{-1}$) were used to estimate the flexibility of the peptide.

2.5. Secondary structure determination

Secondary chemical shift values, short and medium range NOE patterns, and J coupling values were used to assign secondary structures to different regions of Spα1–156, following well established procedures [26,27]. Briefly, α-helices were identified by large positive secondary chemical shifts for C_α and CO and large negative secondary chemical shifts for Hα, medium to strong d_{NN} peaks, the appearance of $d_{\alpha N}(i,i+3)$ or $d_{\alpha N}(i,i+4)$ peaks, and $J_{H\alpha HN}$ values smaller than 6 Hz. Random coil regions were characterized by small secondary chemical shift values (either positive or negative), and $J_{H\alpha HN}$ values greater than 6 Hz. Random coils were also represented by high flexibility with negative or smaller NOE values than other structured parts.

2.6. Molecular modeling

A model structure was generated based on the homologous structure of *Drosophila* spectrin [9,20]. Helix lengths and the positions of the random coils were adjusted to reflect the secondary structure determined in this study. Typically, 100 steps of steepest descent local energy minimization were performed on the resulting structure to remove bad contacts in the vicinity of the adjusted part. The relative orientation of the first helix to the structural domain was arbitrary since the two are connected with a flexible linker. A random coil conformation was generated for the region consisting of residues 1–20.

3. Results

3.1. Folding

Circular dichroism studies indicate that Spα1–156 exhibits a relatively high helical content (41%), suggesting that the peptide is well folded; this is somewhat less than the 52% previously seen for the helical content of Spα52–156 [9], and is consistent with the relatively large random coil segments found in the first 20 residues (see below).

3.2. Solution characterization

It is essential to determine whether the peptide under investigation exists as monomers in NMR solution samples, since the presence of oligomers at high concentration in samples

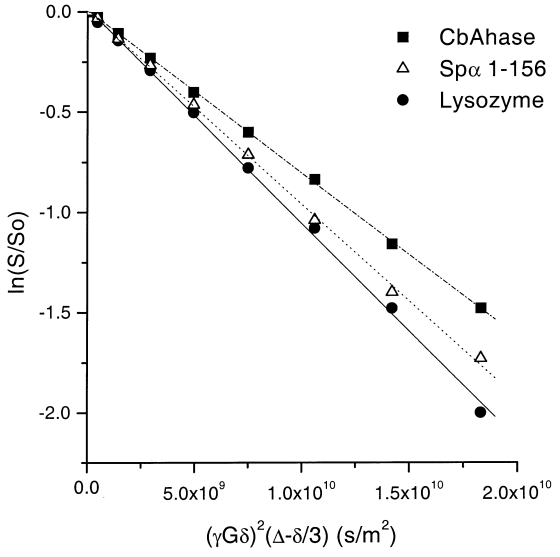

Fig. 1. Diffusion coefficient measurement using PFG-NMR stimulated echo experiment for lysozyme, carbonic anhydrase, and Spα1–156. S/S_O, normalized signal intensity; γ, proton gyromagnetic ratio; G, gradient strength; δ, gradient pulse duration; Δ, diffusion delay. The diffusion coefficients were calculated from the negative of the slopes using the equation, $\ln(S/S_O) = -D_T(\gamma G\delta)^2(\Delta-\delta/3)$ with D_T being the diffusion coefficient.

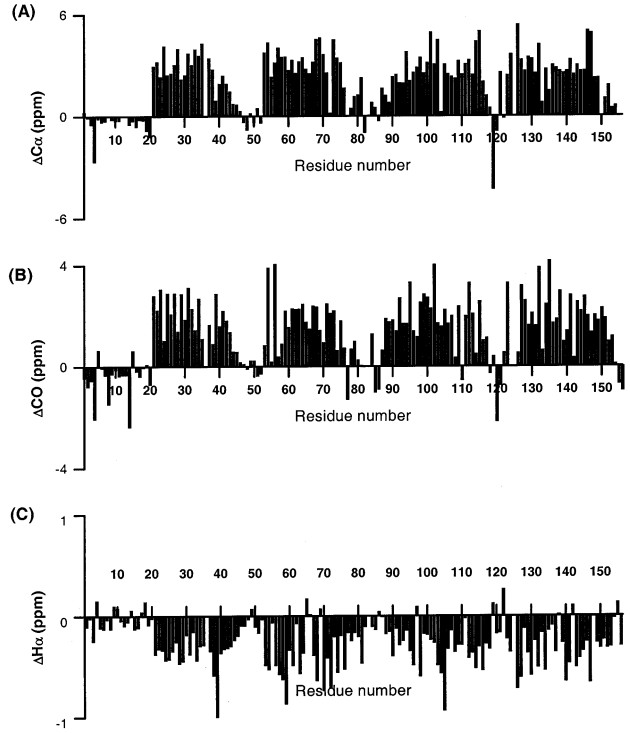

Fig. 2. Secondary chemical shifts of amino acids in Spα1–156. The values represent the chemical shift difference between those of the particular residues and the random coil values. The chemical shifts of the residues were directly referenced against 2,2-dimethyl-2-silapentane-5-sulfonic acid (DSS).

used for NMR studies would pose experimental and analytical complications. Fig. 1 shows the exponential decay of the normalized PFGSE signal intensity as a function of increasing gradient strengths. Lysozyme (14.3 kDa) and carbonic anhydrase (29.0 kDa) were used as reference proteins since they are known to exist as monomers. D_T calculated from the slope was 1.06×10^{-10} m^2/s for lysozyme, in good agreement with published values (1.08×10^{-10} m^2/s) [21], and was 0.81×10^{-10} m^2/s for carbonic anhydrase. The value for Spα1–156 was 0.96×10^{-10} m^2/s, suggesting that the apparent mass for Spα1–156 under these particular solution conditions is larger than 14.3 kDa, but smaller than 29.0 kDa, consistent with the monomeric mass of 18.7 kDa.

3.3. Secondary structure of Spα1–156

From the Spα1–156 backbone resonances assignments [18], the secondary chemical shifts for Cα, CO and Hα of Spα1–156 were obtained (Fig. 2). The *J* coupling constants obtained from amide proton to nitrogen to α-carbon correlation (HNCA)-*J* experiments, and short and medium range NOEs are also shown in Fig. 3. Based on the criteria described above in Section 2, four α-helices were identified, consisting of residues 21–45, 53–81, 88–118 and 123–153. In addition, four random coil regions were identified for residues 1–20, 46–52, 82–87 and 119–122. The last three residues (154–156) also appeared to be in random coil conformation. The random coil character of residues 46–52 was immediately apparent from the resonance assignments since the resonances for these residues appear as very intense peaks and are located in typical random coil regions of the 2D-HSQC spectrum (data not shown).

Thus, the NMR results show that Spα1–156 residues 1–20 exhibit a random coil conformation, followed by an α-helical segment of 25 amino acids (helix C′), followed by another random coil region (residues 46–52). The next 29 residues are α-helical (helix A_1), followed by a 6 residue random coil region (residues 82–87), then a 31 residue α-helical region (residues 88–118, helix B_1), a 4 residue random coil, and a final 31 residue α-helical segment (residues 123–153, helix C_1). As noted previously [28], the exact boundaries of helices in the structure are not clearly defined in some cases. However, the beginning of the first helix (residues 21–45) and of the second helix (residues 53–81) are clearly defined in our system, since criteria used to determine secondary structures change very

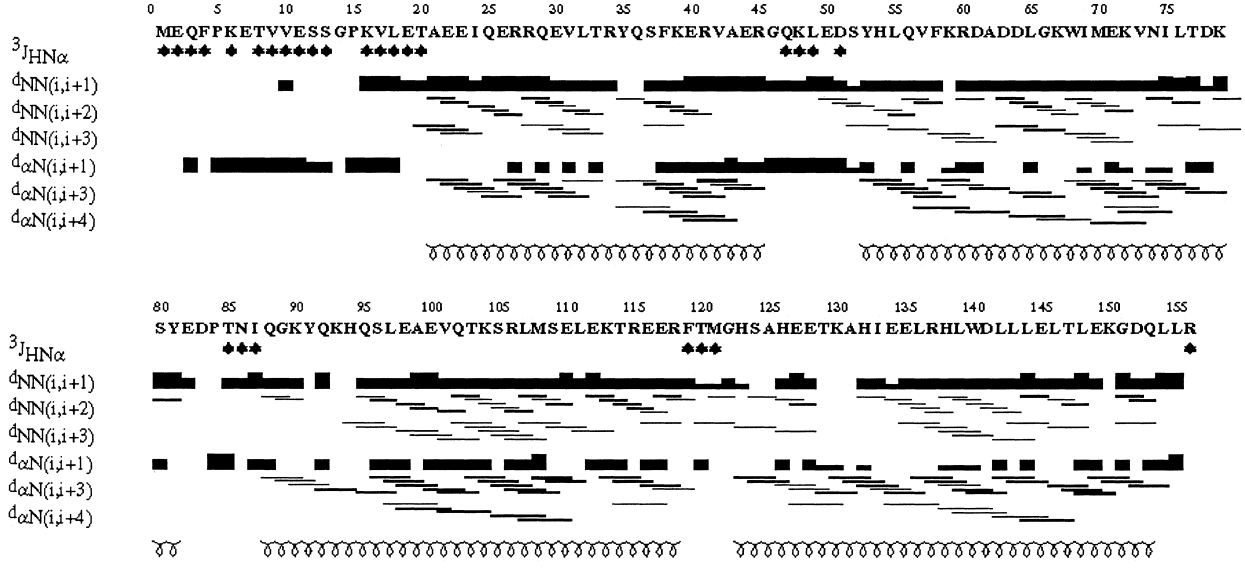

Fig. 3. Summary of short and medium range NOEs and coupling constants for the amino acid residues of Spα1–156. The line widths in NOE rows indicate the relative intensity of NOE peaks for the particular NOE series. The filled stars on the $^3J_{HNa}$ rows indicate three bond coupling constants larger than 6 Hz. Secondary structure elements are depicted as helices at the bottom of each.

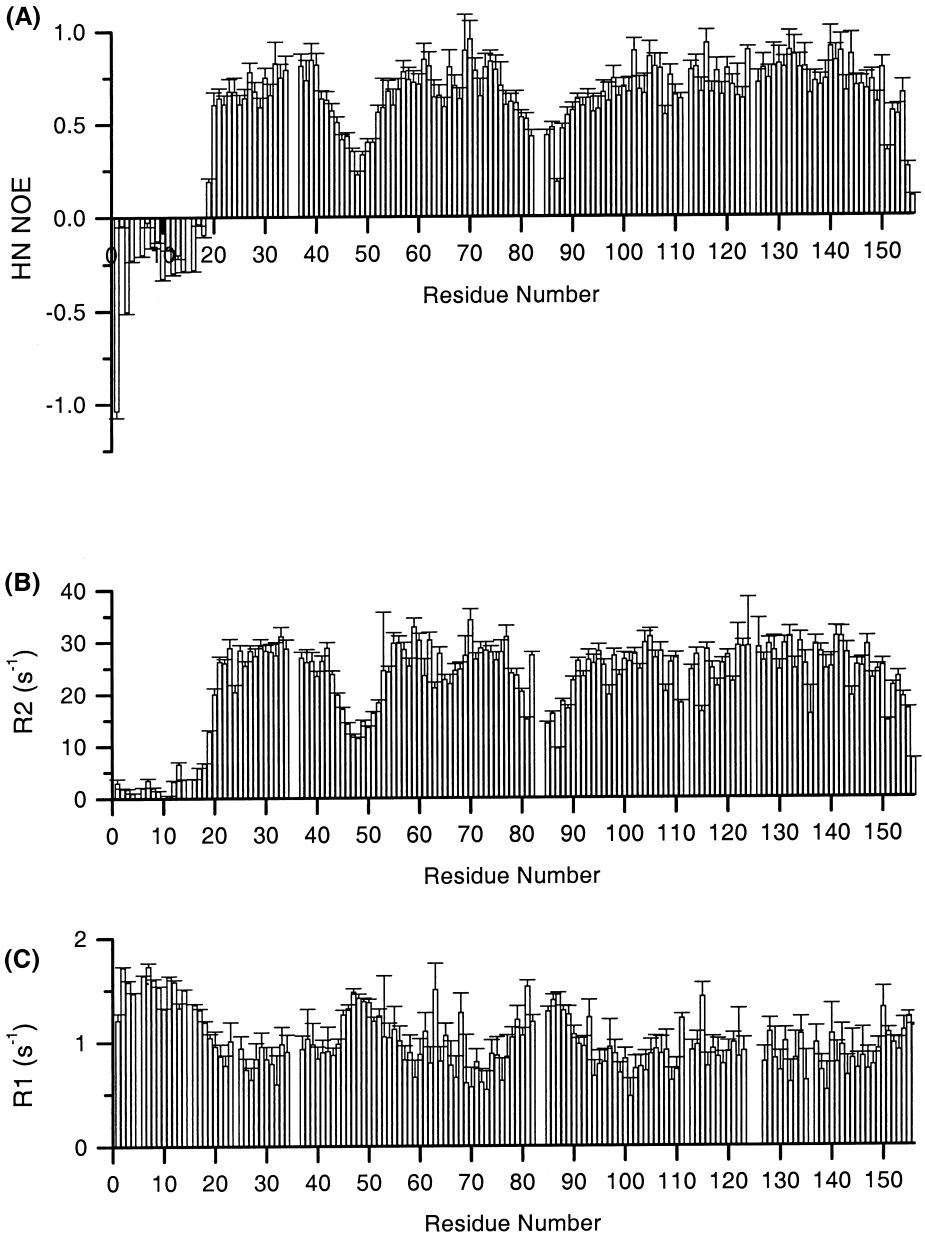

Fig. 4. ^{15}N relaxation measurements for Spα1–156. A: ^{1}H–^{15}N heteronuclear NOE values. B: ^{15}N R_2 values. C: ^{15}N R_1 values. R_1 and R_2 represent the spin lattice and spin spin relaxation rates, respectively. All measurements were done using samples in 150 mM NaCl, 5 mM phosphate, pH 6.5 NMR sample buffer at 20°C in 5% D_2O and 95% H_2O. The relaxation values were obtained from the peak intensities of the appropriate ^{1}H–^{15}N HSQC spectra.

sharply at the boundaries. Thus the first random coil linker region (residues 46–52) is also clearly defined.

Since residues in random coil regions typically exhibit faster internal motion than residues in structured regions, backbone amide ^{15}N relaxation parameters, including the ^{1}H–^{15}N heteronuclear NOE, ^{15}N R_1 values and ^{15}N R_2 values (Fig. 4) were obtained to identify residues exhibiting rapid motions. Residues 1–20 showed negative NOE values, suggesting very rapid motions. Residues 46–52 and 82–87 also had significantly lower NOE values, again suggesting faster internal motion than other residues assigned to helical regions. In addition, the R_2 values of these residues were also significantly larger than those in helical regions, providing further evidence that regions consisting of residues 1–20, 46–52 and 82–87 are random coils. The region with residues 119–122, a region also assigned to random coil structure, did not exhibit an appreciable decrease in NOE values or increase in R_2 values. This feature is discussed later in the text. A model structure based on these secondary structural features was built using the homologous structure of *Drosophila* spectrin [20] and is shown in Fig. 5.

4. Discussion

4.1. Structural domain

Our NMR studies clearly indicate that the first structural domain of human erythrocyte spectrin consists of three helices (helices A_1, B_1 and C_1) connected by two linking segments in

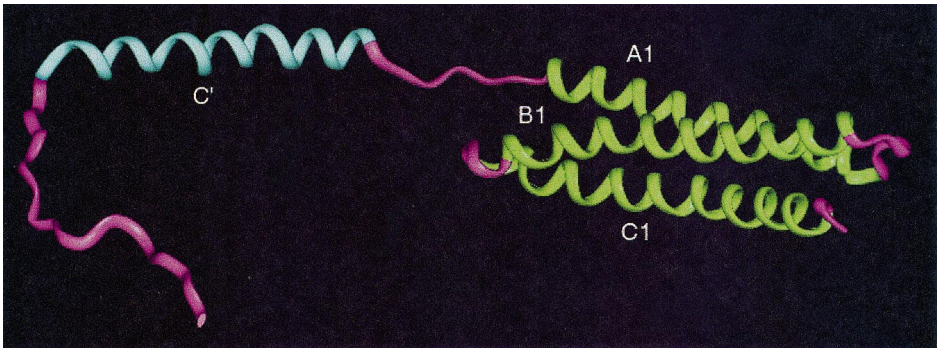

Fig. 5. Model structure of Spα1–156. The model was generated based on secondary structural features reported here and the homologous structure of *Drosophila* spectrin [9,20]. The relative orientation of the first helix to the structural domain is arbitrary since the two are connected with a flexible linker (see text). The helices in the structural domain (A_1, B_1 and C_1) are colored in green, and the helix in the partial domain (C′) is in cyan. All random coils are colored in pink.

random coil conformation. The overall features are in general agreement with previously reported structures of recombinant peptides from *Drosophila* spectrin [20] and from chicken brain spectrin [19,29]. However, there are interesting differences in specific structural features, such as the lengths of helices in structural domains. Each of the three helices in the structural domain of Spα1–156 has a similar length of about 30 residues, consistent with earlier predictions [30]. Other structural domains in human erythrocyte spectrin may have somewhat differing helical lengths, depending on the location of specific domains within the spectrin molecule [30]. In the *Drosophila* spectrin peptide, however, helix A (27 residues) is about eight residues shorter than helix B (34 residues) and four residues shorter than helix C [20]. In chicken brain spectrin, helix A (with 21 residues [29] or 22 residues [19]) is about 14 or 15 residues shorter than helix B (35 residues [19] or 37 residues [29]). Helix C consists of 26 residues [31] or 29 residues [29]. This large difference in lengths between helices A and B leads to the formation of a double helical at the beginning of the structural domain in chicken brain spectrin bundle, instead of a triple helical bundle [29]. However, our data for Spα1–156 show helices A_1, B_1 and C_1 exhibiting similar lengths, which might conveniently form a triple helical bundle.

Our data also indicate that the region between helices B_1 and C_1, consisting of residues 119–122, does not exhibit relatively fast internal motion, with no significant decrease in heteronuclear NOE around residue 121. Since our current data could not distinguish between random coil and tight turn, it is possible that this region in Spα1–156 forms a tight turn, similar to the linker region in chicken brain spectrin, which forms a tight turn between helices B and C [31].

4.2. *Secondary structure of the αN-terminal region prior to the first structural domain*

Probably the most significant finding of this work is the determination of the secondary structure of the first 51 residues – the region prior to the first structural domain in intact spectrin, and the region involved in spectrin tetramerization. Our data clearly show that this region includes an α-helix that is about 26 residues long (helix C′) and a short random coil linker connecting helix C′ to helix A_1 of the first structural domain. It is interesting to find a fully formed helix prior to the first structural domain in Spα1–156 in the absence of its partner, the C-terminal region of β-spectrin. Although it has long been suggested that, in the $\alpha_2\beta_2$ tetramer, two partial domains (one helix from α-spectrin and two helices from β-spectrin) form a triple helical bundle [15,32], there has been no direct information on the structure of this region of spectrin. In fact, a recent report suggested that the partial domain in α-spectrin is partly or largely in random coil conformation which would convert into helix upon binding to β-spectrin [33]. However, our NMR secondary structure analysis clearly shows the presence of a 26 residue long helix in this region. The monomeric state of the peptide, as determined by our diffusion coefficient measurements, excludes any intermolecular interaction that might affect or change the conformation of the region at the high sample concentrations used in the NMR studies. It is not feasible to obtain information on the orientation of helix C′ relative to the structural domain from the NMR data. Thus helix C′ may extend from the structural domain, as shown in Fig. 5, or could bundle with the structure domain to form a four helical bundle structure. To distinguish between these possibilities, we have changed residue 154 to a cysteine residue and labeled it with a paramagnetic spin label, and found that only the residues in the structural domain near residue 154, but not those in helix C′, were unambiguously bleached by the paramagnetic center (data not shown). This suggests that helix C′ does not bundle with the structural domain to form a four helical bundle, but remains as an unpaired helix, as shown in Fig. 5. It seems likely that helix C′ exhibits free rotation about the random coil linker region, rather than protruding rigidly from the structure domain.

Another interesting feature is that helix C′ is linked to helix A_1 of the structure domain through a random coil of seven residues (residues 46–52), resulting in a structure that differs from the structure recently reported for chicken brain spectrin peptides [29], in which helix A_n immediately follows helix C_{n-1} to give a long, continuous and somewhat rigid helix. This long rigid helical structure has been suggested for erythrocyte spectrin [34]. However, from the backbone ^{15}N relaxation measurements, this region exhibits lower NOE and larger R_2 values than other structured regions, indicating that fast motion in residues 46–52 region is evident in our peptide (Fig. 4). Although detailed quantitative analysis of the relaxation data has not yet been done due to the presumed anisotropy, we estimate the internal motions of this linker region (residues 46–52) to be in the ps to ns time scale range, based on the heteronuclear NOE data and the overall correlation time of 11.7 ns, derived from the above mentioned diffusion coefficients. Other studies supporting the feature of a flexible linker

include secondary structure prediction [30] and electric birefringence measurements [35]. In addition, hinge segments with high sensitivity to proteolysis were considered to be responsible for the flexibility of another spectrin-like molecule, dystrophin in muscle [36]. This random coil linker conformation suggests that there might be different flexibility mechanisms from those suggested for chicken brain spectrin, depending on the position or the source of the particular spectrin domains. If this random coil linker is a common feature between two structural domains, then erythrocyte spectrin may exhibit substantial flexibility, in good agreement with our earlier findings on the detection of segmental motions in intact spectrin [37,38]. Confirmation of the general presence of random coil linkers in other parts of human erythrocyte spectrin awaits experiments on peptides from other regions of spectrin.

Acknowledgements: This research was supported in part by the following Grants: NSF MCB 9801870 (to L.W.-M.F.), NIH HL57604 and American Heart Association Midwest Affiliate (to M.E.J.) and an American Heart of Association Midwest Affiliate pre-doctoral fellowship (to S.P.). This research made use of the National Magnetic Resonance Facility at the University of Wisconsin, Madison, which is supported by NIH Grant RR02301 from the Biomedical Research Technology Program, National Center for Research Resources. Equipment in the facility was purchased with funds from the University of Wisconsin, NFS (DMB-8415048 and BIR-9214394), NIH (RR02301, RR02781 and RR08438) and the US Department of Agriculture.

References

[1] Bennett, V., Davis, J., Gardner, K. and Steiner, J.P. (1988) Soc. Gen. Physiol. Ser. 43, 101–109.
[2] Shimizu, T., Takakuwa, Y., Koizumi, H., Ishibashi, T. and Ohkawara, A. (1996) Arch. Dermatol. Res. 288, 19–23.
[3] Goodman, S.R., Krebs, K.E., Whitfield, C.F., Riederer, B.M. and Zagon, I.S. (1988) CRC Crit. Rev. Biochem. 23, 171–234.
[4] Viel, A. (1999) FEBS Lett. 460, 391–394.
[5] Weber, I., Niewohner, J. and Faix, J. (1999) Biochem. Soc. Symp. 65, 245–265.
[6] Dubreuil, R.R. and Grushko, T. (1998) BioEssays 20, 875–878.
[7] Speicher, D.W. and Marchesi, V.T. (1984) Nature 311, 177–180.
[8] Dhermy, D. (1991) Biol. Cell 71, 249–254.
[9] Menhart, N., Mitchell, T., Lusitani, D., Topouzian, N. and Fung, L.W.-M. (1996) J. Biol. Chem. 271, 30410–30416.
[10] Pascual, J., Castresana, J. and Saraste, M. (1997) BioEssays 19, 811–817.
[11] Leto, T.L., Pleasic, S., Forget, B.G., Benz Jr., E.J. and Marchesi, V.T. (1989) J. Biol. Chem. 264, 5826–5830.
[12] Mikkelsen, A., Stokke, B.T. and Elgsaeter, A. (1984) Biochim. Biophys. Acta 786, 95–102.
[13] Ralston, G.B. (1991) Biochemistry 30, 4179–4186.
[14] Delaunay, J. and Dhermy, D. (1993) Semin. Hematol. 30, 21–33.
[15] Tse, W.T., Lecomte, M.C., Costa, F.F., Garbarz, M., Feo, C., Boivin, P., Dhermy, D. and Forget, B.G. (1990) J. Clin. Invest. 86, 909–916.
[16] Cherry, L., Menhart, N. and Fung, L.W.-M. (1999) J. Biol. Chem. 274, 2077–2084.
[17] Lusitani, D.M., Qtaishat, N., LaBrake, C.C., Yu, R.N., Davis, J., Kelley, M.R. and Fung, L.W.-M. (1994) J. Biol. Chem. 269, 25955–25958.
[18] Park, S., Liao, X., Johnson, M.E. and Fung, L.W.-M. (1999) J. Biomol. NMR 15, 345–346.
[19] Pascual, J., Pfuhl, M., Walther, D., Saraste, M. and Nilges, M. (1997) J. Mol. Biol. 273, 740–751.
[20] Yan, Y., Winograd, E., Viel, A., Cronin, T., Harrison, S.C. and Branton, D. (1993) Science 262, 2027–2030.
[21] Altieri, A.S., Hinton, D.P. and Byrd, R.A. (1995) J. Am. Chem. Soc. 117, 7566–7567.
[22] Ilyina, E., Roongta, V., Pan, H., Woodward, C. and Mayo, K.H. (1997) Biochemistry 36, 3383–3388.
[23] Farrow, N.A., Muhandiram, R., Singer, A.U., Pascal, S.M., Kay, C.M., Gish, G., Shoelson, S.E., Pawson, T., Forman-Kay, J.D. and Kay, L.E. (1994) Biochemistry 33, 5984–6003.
[24] Palmer, A.G., Rance, M. and Wright, P.E. (1991) J. Am. Chem. Soc. 113, 4371–4380.
[25] Skelton, N.J., Palmer, A.G., Akke, M., Koerdel, J. and Rance, M. (1993) J. Magn. Res. Ser. B 102, 253–264.
[26] Wuthrich, K. (1986) NMR of Proteins and Nucleic Acids, John Wiley and Sons, New York.
[27] Spera, S. and Bax, A. (1991) J. Am. Chem. Soc. 113, 5490–5492.
[28] Ikura, M., Spera, S., Barbato, G., Kay, L.E., Krinks, M. and Bax, A. (1991) Biochemistry 30, 9216–9228.
[29] Grum, V.L., Li, D., MacDonald, R.I. and Mondragon, A. (1999) Cell 98, 523–535.
[30] Speicher, D.W., Davis, G. and Marchesi, V.T. (1983) J. Biol. Chem. 258, 14938–14947.
[31] Pascual, J., Pfuhl, M., Rivas, G., Pastore, A. and Saraste, M. (1996) FEBS Lett. 383, 201–207.
[32] Speicher, D.W., DeSilva, T.M., Speicher, K.D., Ursitti, J.A., Hembach, P. and Weglarz, L. (1993) J. Biol. Chem. 268, 4227–4235.
[33] Lecomte, M.C., Nicolas, G., Dhermy, D., Pinder, J.C. and Gratzer, W.B. (1999) Eur. Biophys. J. 28, 208–215.
[34] Parry, D.A., Dixon, T.W. and Cohen, C. (1992) Biophys. J. 61, 858–867.
[35] Bjorkoy, A., Mikkelsen, A. and Elgsaeter, A. (1999) Biochim. Biophys. Acta 1430, 323–340.
[36] Koenig, M. and Kunkel, L.M. (1990) J. Biol. Chem. 265, 4560–4566.
[37] Fung, L.W.-M., Lu, H.Z., Hjelm Jr., R.P. and Johnson, M.E. (1986) FEBS Lett. 197, 234–238.
[38] Fung, L.W.-M., Lu, H.Z., Hjelm Jr., R.P. and Johnson, M.E. (1989) Life Sci. 44, 735–740.